INT6 interacts with MIF4GD/SLIP1 and is necessary for efficient histone mRNA translation

JULIA NEUSIEDLER,[1,3,4] VINCENT MOCQUET,[1,3] TARAN LIMOUSIN,[2] THEOPHILE OHLMANN,[2] CHRISTELLE MORRIS,[1] and PIERRE JALINOT[1,5]

[1]Laboratoire de Biologie Moléculaire de la Cellule, Unité Mixte de Recherche 5239, Centre National de la Recherche Scientifique, Ecole Normale Supérieure de Lyon, 69364 Lyon cedex 07, France
[2]Virologie Humaine, Unité 758, Institut National de la Santé et de la Recherche Médicale, Ecole Normale Supérieure de Lyon, 69364 Lyon cedex 07, France

ABSTRACT

The INT6/EIF3E protein has been implicated in mouse and human breast carcinogenesis. This subunit of the eIF3 translation initiation factor that includes a PCI domain exhibits specific features such as presence in the nucleus and ability to interact with other important cellular protein complexes like the 26S proteasome and the COP9 signalosome. It has been previously shown that INT6 was not essential for bulk translation, and this protein is considered to regulate expression of specific mRNAs. Based on the results of a two-hybrid screen performed with INT6 as bait, we characterize in this article the MIF4GD/SLIP1 protein as an interactor of this eIF3 subunit. MIF4GD was previously shown to associate with SLBP, which binds the stem–loop located at the 3′ end of the histone mRNAs, and to be necessary for efficient translation of these cell cycle–regulated mRNAs that lack a poly(A) tail. In line with the interaction of both proteins, we show using the RNA interference approach that INT6 is also essential to S-phase histone mRNA translation. This was observed by analyzing expression of endogenous histones and by testing heterologous constructs placing the luciferase reporter gene under the control of the stem–loop element of various histone genes. With such a reporter plasmid, silencing and overexpression of INT6 exerted opposite effects. In agreement with these results, INT6 and MIF4GD were observed to colocalize in cytoplasmic foci. We conclude from these data that INT6, by establishing interactions with MIF4GD and SLBP, plays an important role in translation of poly(A) minus histone mRNAs.

Keywords: histone mRNA; translation; MIF4GD; INT6; eIF3; SLBP

INTRODUCTION

The *INT6* gene was originally characterized as an integration site of the Mouse Mammary Tumor Virus (MMTV) in one preneoplastic mammary hyperplastic outgrowth line and two independent mammary tumors arising in unrelated mice (Marchetti et al. 1995). The human INT6 protein was further identified as a target of the Human T-cell Leukaemia Virus type 1 (HTLV-1) transforming protein Tax (Desbois et al. 1996) and also as the EIF3E subunit of the eIF3 translation initiation factor (Asano et al. 1997). EIF3 establishes multiple contacts with other translation initiation factors like eIF1A, eIF5, and eIF4G (Hinnebusch 2006; Hershey 2010). It also binds the mRNA, the 40S ribosome subunit, and favors association with the ternary complex, thereby playing a key role in translation initiation. The general structure of eIF3 has been analyzed by electronic microscopy and revealed a five-lobe organization (Siridechadilok et al. 2005). INT6 includes in its C-terminal part a proteasome–COP 9 signalosome–initiation of translation (PCI) domain, which is also present in several subunits of the proteasome 19S regulatory particle, of the COP9 signalosome (CSN), and of eIF3. The PCI subunits of these complexes, which are involved in protein degradation, SCF E3 ubiquitin ligase regulation, and mRNA translation, respectively, are likely to play a scaffold role (Pick et al. 2009). Intriguingly, INT6 has also been characterized to interact with several subunits of the proteasome and of the CSN and to associate in vivo with these complexes, although in lesser amounts as compared with eIF3 (Karniol et al. 1998; Yahalom et al. 2001; Hoareau Alves et al. 2002; Yen et al. 2003). In line with such interactions, INT6 has been reported to control the stability of specific cellular proteins. Indeed, we and others have previously shown that it acts positively on the stability of the MCM7 subunit of the DNA replication licensing factor MCM by interacting

[3]These authors contributed equally to this work.
[4]**Present address:** Wellcome Trust Centre for Gene Regulation and Expression, University of Dundee, Dundee DD1 5EH, UK.
[5]**Corresponding author.**
E-mail pjalinot@ens-lyon.fr.
Article published online ahead of print. Article and publication date are at http://www.rnajournal.org/cgi/doi/10.1261/rna.032631.112.

with its polyubiquitinylated forms (Buchsbaum et al. 2007; Grzmil et al. 2010). Conversely, Chen et al. (2007, 2010) have shown that INT6, by binding to HIF-2α, triggers its proteolytic degradation. INT6 has also been shown to negatively control the stability of the steroid coreceptor 3 (SRC3) during mitosis (Suo et al. 2011). Besides these activities on protein stability, INT6 has also been shown to intervene in translation; however, its effect seems restricted to specific proteins. Indeed, both in fission yeast and in mammalian cells, knockdown of INT6 does not appear to modify significantly incorporation of ^{35}S-labeled methionine in proteins or polysome profile (Bandyopadhyay et al. 2000; Zhou et al. 2005; Grzmil et al. 2010). This has been reported by different groups and corresponds to our own observations. However, current data do not exclude more specific activities of INT6 in this process. Indeed, Zhou et al. (2005) have reported that two kinds of eIF3 complexes exist in fission yeast, one characterized by the presence of eIF3m and the other by that of eIF3e. This latter type was found associated with a limited set of specific mRNAs. In a previous study, we have also established that INT6 was required in human cells for the efficiency of the nonsense-mediated mRNA decay pathway (NMD), which prevents expression of truncated proteins that can exert deleterious effects (Morris et al. 2007). This activity is correlated with the ability of INT6 to interact with specific NMD factors like UPF1 and UPF2. It has also been recently reported that INT6 was able to act positively or negatively on the translation of specific mRNAs as evaluated by their presence in high-molecular-weight polysomes (Grzmil et al. 2010). From these various observations, the picture emerges that INT6 selectively acts on translation in either a positive or negative way (Grzmil et al. 2010), but the exact underlying molecular mechanisms remain to be characterized.

A specific feature of the protein-coding mRNAs is the poly(A) tail at their 3′ end that binds several proteins including the poly(A) binding protein (PABP), which plays an important role in translation by creating interactions with initiation factors such as eIF4G and thereby causes circularization of the mRNA molecule (Amrani et al. 2008; Martineau et al. 2008). However, one family of cellular mRNAs lacks a poly(A) tail: that expressing the five classes of histone (H1, H2A, H2B, H3, and H4). Instead of the poly(A) signal, these specific mRNAs include near their 3′ end a 16-nt stem–loop that interacts with the SLBP protein that plays a key role in the metabolism of these RNAs (Zhao et al. 2004; Townley-Tilson et al. 2006). Indeed, this protein forms a complex with other factors including symplekin and ZFP100, which in combination with the U7 mRNP and CSPF73 trigger cleavage of the histone mRNA a few nucleotides after the stem–loop (Dominski et al. 2005; Kolev and Steitz 2005; Kolev et al. 2008; Sullivan et al. 2009b). This implies a hybridization between the 5′ part of the U7 RNA and the HDE element that is located downstream from the stem–loop (Dominski and Marzluff 2007). Besides its role in formation of the 3′ end, SLBP is also important for export of the histone mRNA (Ghule et al. 2008; Sullivan et al. 2009a), as well as for their productive translation, and this translational activity relies on interactions with eIF4G and eIF3 translation initiation factors (Ling et al. 2002; Gorgoni et al. 2005). More recently, it has also been reported that this effect involves an interaction with a protein identified in a two-hybrid screen performed with SLBP as bait, which was accordingly named SLBP interacting protein 1 (SLIP1) (Cakmakci et al. 2008). This small 25-kDa protein corresponds almost entirely to a middle domain of eukaryotic initiation factor 4G (MIF4G) and has been designated accordingly as MIF4G domain-containing protein (MIF4GD) by the HUGO Gene Nomenclature Committee, which name is further used in this article. After completion of DNA replication and ending of the S phase during which histone genes are expressed, SLBP plays a role in degradation of the histone mRNAs and is itself further degraded by the ubiquitin proteasome pathway (Kaygun and Marzluff 2005). From the current data, it clearly appears that SLBP plays a pivotal role in the metabolism of the histone mRNAs that are issued from the most cell cycle–regulated cellular genes, their S-phase-specific expression relying on regulation at the transcriptional, maturation, and translational steps.

In this study, we identified an unanticipated interaction between INT6 and the MIF4GD protein. In line with this association, we observed that INT6 is required for efficient translation of the histone mRNAs during S phase. Our data support a novel specific role of this proto-oncoprotein in the translation of this specific type of cellular mRNA.

RESULTS

Interaction between INT6 and MIF4GD

A two-hybrid screen was performed with INT6 as bait using a cDNA library of immortalized human B lymphocytes. This screen led to the identification of several INT6 interactors such as RFP, MCM7, and several subunits of the eIF3 complex, of the CSN, and of the 19S proteasome regulatory particle as previously reported (Morris-Desbois et al. 1999; Hoareau Alves et al. 2002; Buchsbaum et al. 2007). Among the clones obtained in this screen, three encoded MIF4GD. One clone, THI 22, included the complete MIF4GD coding sequence, while the other two lacked the first 16 N-terminal amino acids (Fig. 1A). After isolation from yeast and retesting against the INT6 bait, all three clones were positive (Fig. 1A). To further test the interaction between both proteins in human cells, a vector expressing the complete MIF4GD coding sequence fused to the HA epitope at the C-terminal end was constructed. HeLa cells were transfected with this MIF4GDHA expression vector together with either a control plasmid or a construct expressing INT6 fused to the Flag epitope at its C-terminal end. Immunoprecipitation

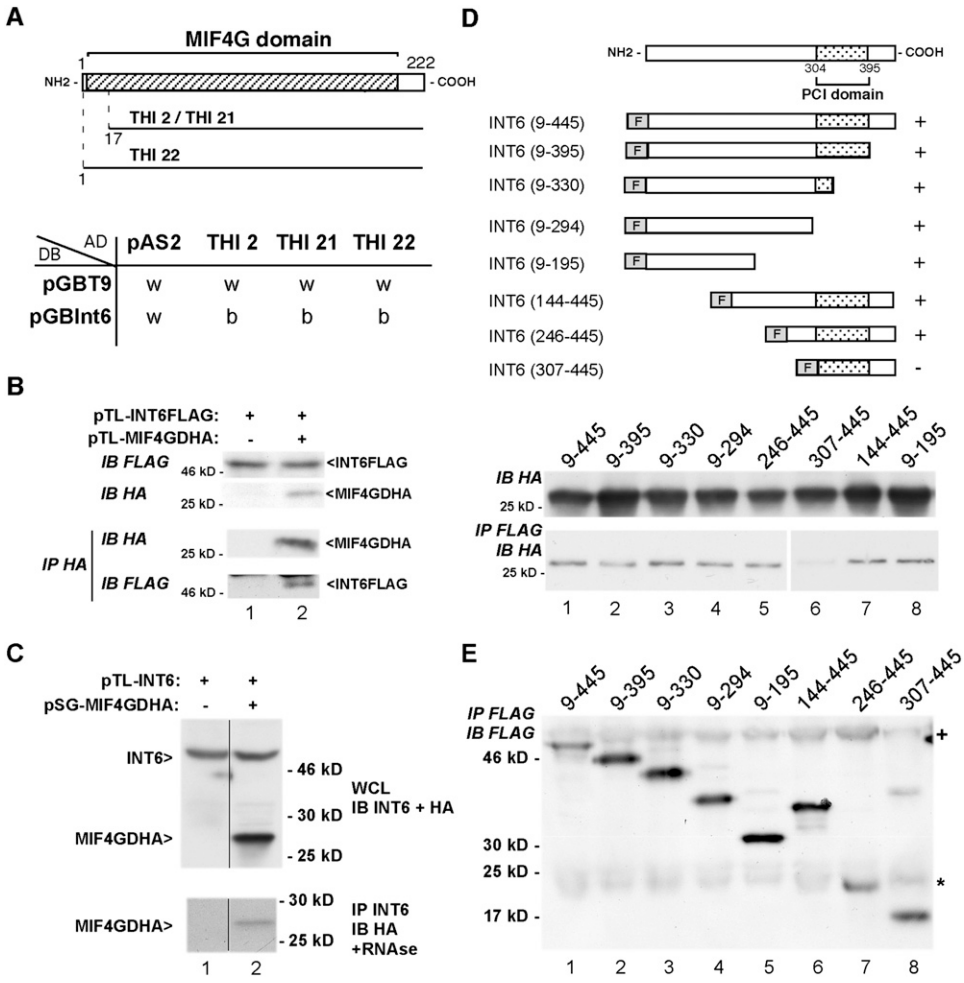

FIGURE 1. The MIF4GD protein interacts with INT6. (*A*) Schematic representation of the three clones encoding MIF4GD identified by two-hybrid screen with INT6 as bait. The table represents the results of testing these clones by two-hybrid with vectors expressing the GAL4 DNA binding domain alone (pGBT9) or in fusion with INT6 (pGBInt6). As control, the assay was also performed with a vector expressing the GAL4 activation domain alone (pAS2). The letters w (white) and b (blue) indicate the color of the colonies after 24 h. (*B*) HeLa cells were transfected with the pTL1-INT6FLAG construct, alone (lane *1*) or together with the MIF4GDHA expression vector (lane *2*). To monitor expression, cell lysates were analyzed by immunoblot with antibodies to Flag (*top* panel) and to HA (second panel from *top*). Cell lysates were immunoprecipitated with the antibody to HA, and precipitated proteins were analyzed by immunoblot using the antibody to Flag (*bottom* panel) and to HA to verify efficiency of immunoprecipitation (third panel from *top*). (*C*) COS7 cells were transfected with the pTL-INT6 (lanes *1* and *2*) and pSG-MIF4GDHA (lane *2*) expression vectors. Whole cell lysates were analyzed by immunoblot using a mix of antibodies to INT6 and HA (*top* panel). These lysates were used to perform immunoprecipitation using the antibody to INT6 (C20) in the presence of RNAse A. Immunoprecipitates were analyzed by immunoblot using the monoclonal antibody to HA (*bottom* panel). The positions of the INT6 and MIF4GDHA signals are indicated. (Vertical black line) The two represented lanes were from the same blot but not in adjacent lanes. (*D*) Schematic representation of several INT6 deletion mutants fused to the Flag epitope. COS7 cells were transfected with the MIF4GDHA expression vector together with the constructs expressing the various parts of INT6 fused to Flag as indicated. Lysates of these cells were used to perform immunoprecipitations with the antibody to Flag and immunoblot analysis with the antibody to HA. (*E*) The Flag immunoprecipitates of panel *D* were analyzed by immunoblot using a monoclonal antibody to Flag. The star and the cross on the *right* indicate nonspecific bands corresponding to the immunoglobulin heavy and light chains. The positions of the bands of a molecular weight marker run in parallel are indicated on the *left*.

using the antibody to HA showed a coprecipitation of INT6FLAG with SLIPHA (Fig. 1B, bottom panel). The same experiment was performed with a vector expressing untagged INT6 and in the presence of RNAse. Under these conditions, MIF4GDHA was also coprecipitated with the antibody to INT6 (Fig. 1C, lane 2). The experiment was also performed in the reverse way by transfecting cells with constructs expressing various parts of INT6 fused to the Flag epitope at their N-terminal end together with the vector expressing MIF4GDHA. Immunoprecipitation experiments using an antibody to Flag followed by an immunoblot with the antibody to HA revealed binding of MIF4GD to all INT6 mutants (Fig. 1D, bottom panel), except that corresponding roughly to the C-terminal PCI domain (Fig. 1D, lane 6). All of these INT6 mutants were precipitated in similar amounts (Fig. 1E). This indicated that the PCI

domain of INT6 is not involved in the interaction and that MIF4GD interacts with different regions of the N-terminal part of INT6 as it binds with similar efficiencies the 9–195 and 246–445 INT6 mutants. These results established that INT6 binds MIF4GD in human cells through its N-terminal part.

INT6 is necessary for efficient translation of histone mRNAs in S phase

It has been reported previously that MIF4GD interacts with SLBP and is required for efficient translation of histone mRNAs (Cakmakci et al. 2008). Because INT6 is associated with the eIF3 translation initiation complex and binds MIF4GD, we next examined whether INT6 is also important for histone mRNA translation. To this end, HeLa cells were transfected with siRNAs, either control or directed against INT6 or MIF4GD and synchronized in S phase by a double-thymidine block (Fig. 2A). The efficiency of silencing was checked by RNA and protein analysis (Supplemental Fig. S1A,B). To control whether silencing of these proteins affects cell cycle distribution of the synchronized cells, a flow cytometry analysis was carried out. Due to synchronization, the majority of the cells were indeed in S phase, and this was not significantly modified by transfection of the *INT6* or *MIF4GD* siRNAs duplexes (Supplemental Fig. S2), although with the latter one a decrease in G_1 cells correlated with a higher percentage of cells in G_2/M (Supplemental Fig. S2). Three hours after second block release, cells were incubated with ^{35}S-labeled methionine and cysteine for 10 min, and the histones were purified by acidic extraction. After electrophoretic separation, the gel was first stained with Coomassie Blue (Supplemental Fig. S1C) showing the four canonical histones. Radioactivity was then analyzed with a phosphorimager (Fig. 2B). This allowed detection of histones H3, H2B, and H4, but not H2A, which lacks internal methionine or cysteine. With three different *INT6* siRNAs as well as with *MIF4GD* siRNAs, a reduction of the radioactivity incorporated in the three canonical histones was observed (Fig. 2B, cf. lane 1 with lanes 2–5). This experiment was repeated three times, and the radioactivity in the histone signals was normalized with bands of the upper part of the gel (Cakmakci et al. 2008). Because they were poorly separated, the bands corresponding to histones H2B and H3 were grouped for quantification. After this normalization, it was observed that silencing of MIF4GD and INT6 led to similar reduction of radioactivity incorporation in histones (Fig. 2C). As previously shown, this decrease was not due to a lower percentage of cells in S phase (Supplemental Fig. S2). To verify further that this reduction was due to a translational effect, the amount of histone H2B, H3, and H4 mRNAs was analyzed by Northern blot. Silencing of INT6 and MIF4GD was not observed to decrease the signals corresponding to these mRNAs (Fig. 3A,B). Because

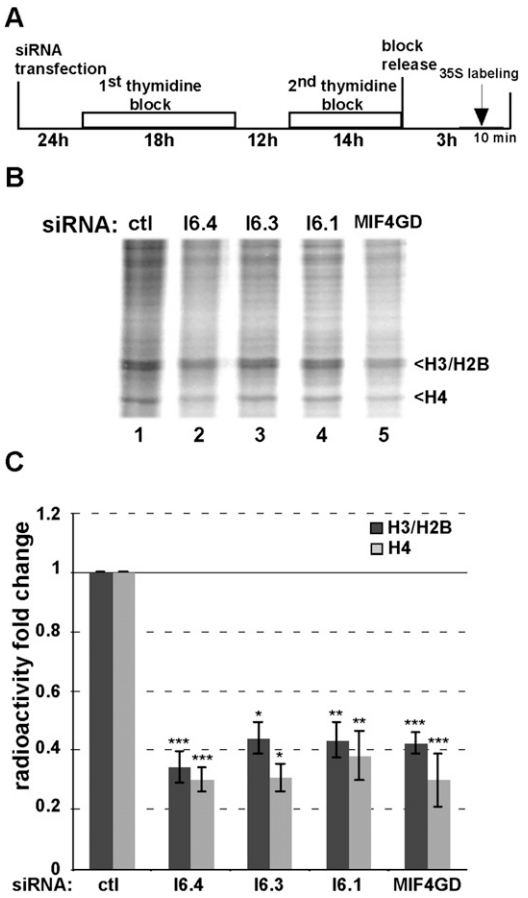

FIGURE 2. Effect of INT6 knockdown on histone protein synthesis. (*A*) Schematic representation of the protocol used to synchronize cells and to label histones. HeLa cells were synchronized by a double-thymidine block and released into the S phase after the second block. Cells were then pulse-labeled for 10 min with ^{35}S-labeled methionine and cysteine. (*B*) HeLa cells were transfected with either control (lane *1*) or three different siRNA duplexes targeting INT6 (lanes *2–4*) or *MIF4GD* siRNAs (lane *5*). The proteins obtained after acidic extraction were separated on a 15% SDS-polyacrylamide gel, and radioactivity was analyzed using a phosphorimager. The bands corresponding to histones H3, H2B, and H4 are indicated. (*C*) The experiment was repeated three times, and the amount of radioactivity in the H3/H2B bands as well as in the H4 band was quantified using the MultiGauge software with normalization with respect to bands of the upper part of the gels as previously described (Cakmakci et al. 2008). The mean of the ratios with respect to cells transfected with control siRNAs is represented with an error bar corresponding to the standard deviation. Data were analyzed with a Student's *t*-test (two-tailed, unpaired), and the stars indicate a *P*-value of (*) <0.05, (**) 0.01, or (***) 0.001 with respect to the control siRNA condition.

there are multiple copies of histone genes in the human genome, this method did not allow distinction between specific H2B, H3, and H4 genes. Hence, a more precise analysis was performed using the NanoString technology with probes designed to be gene-specific. These were usually located in the region upstream of the stem–loop, which is poorly conserved among the various histone genes. Such probes were designed for most of the histone genes, except those that are highly tissue-specific, such as genes

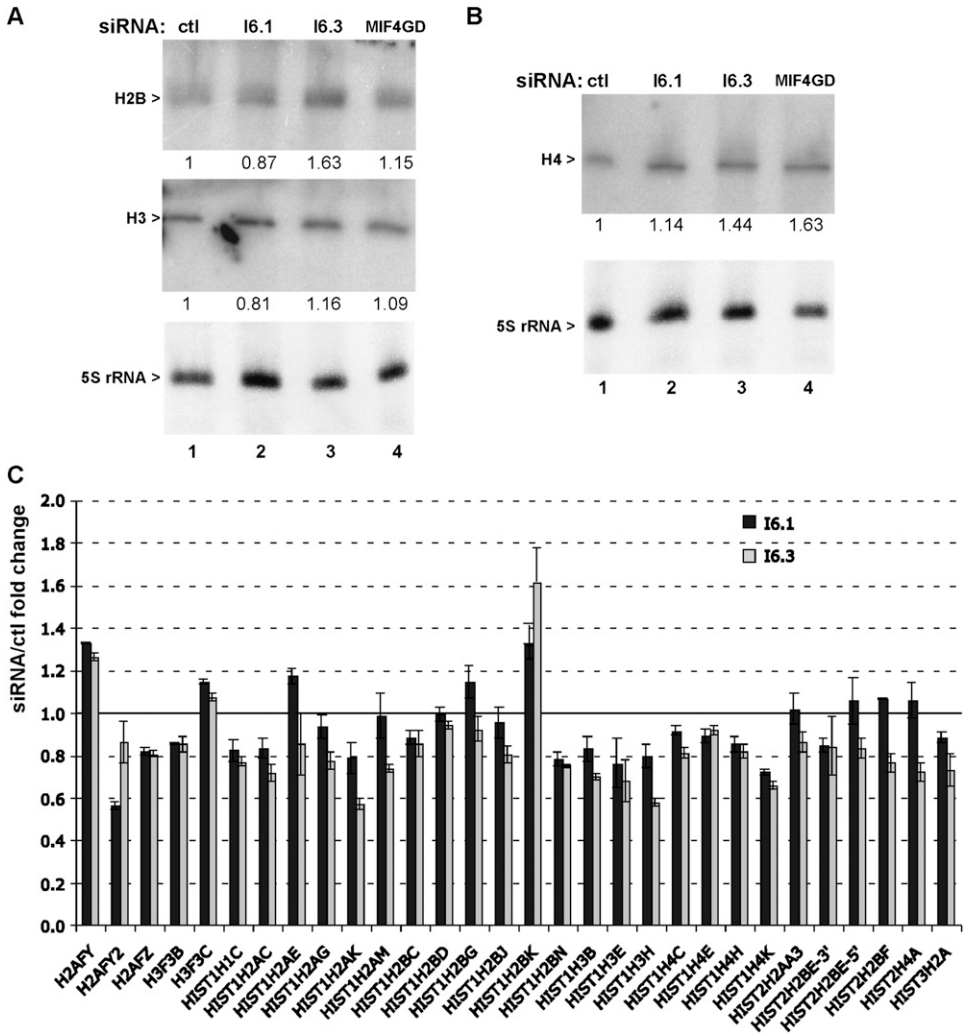

FIGURE 3. Analysis of H2B, H3, and H4 mRNAs by Northern blot and gene-specific quantification of histone mRNA levels using the NanoString technology. (*A*,*B*) HeLa cells were tranfected with control, I6.1, I6.3, or *MIF4GD* siRNAs, and total RNAs were purified and separated on a polyacrylamide gel. The gel was stained with ethidium bromide, and the signal corresponding to 5S rRNA is shown as the loading control (*bottom* panels). After transfer to nylon membranes, hybridization was performed with an oligonucleotide corresponding to a region highly conserved among H3 genes on the antisense strand (*A*, *middle* panel). The membrane was stripped and hybridized again with an H2B probe (*A*, *top* panel). The same experiment with another gel was performed using an H4 probe (*B*, *top* panel). Numbers *below* the blot are the fold change with respect to control siRNAs after quantification and normalization with respect to 5S RNA. (*C*) HeLa cells were transfected with control, I6.1, or I6.3 siRNAs. Total RNAs were prepared and quantified with the nCounter apparatus using probes specific to the histone genes indicated, as well as of *EIF3E* and *MIF4GD* mRNA. The graph represents the mean of either two (I6.1, dark gray) or three (I6.3, light gray) independent experiments as ratio with respect to control siRNA; error bars indicate the standard deviation.

expressed in the testis. In this list were also included seven normalization genes, as well as a probe specific to INT6. Although *INT6* mRNA was strongly reduced by siRNA transfection (Supplemental Fig. S1A) as expected, expression of the various histone genes was generally only slightly affected by INT6 silencing (Fig. 3C). This was also the case for *MIF4GD* siRNA transfection (data not shown). Hence, it appears that INT6 silencing does significantly reduce translation of mRNAs coding for canonical histones during S phase and that this effect does not result from a comparable decrease in mRNA amounts. In this analysis, the effects of INT6 and MIF4GD were found to be similar.

To confirm this point, another approach was undertaken. The firefly luciferase cDNA was placed under the control of the promoter and stem–loop sequence of various genes coding for canonical histones (Fig. 4A). The sequence including the stem–loop extended in the 3′ part to include the complete HDE. Such constructs were generated using these regulatory elements of the *HIST1H2AC*, *HIST1H2BG*, and *HIST2H4A* genes. These vectors were transfected together with a control plasmid expressing the *Renilla* luciferase, and these experiments were performed in cells silenced for INT6 or MIF4GD by cotransfection of corresponding siRNAs. Transfections were repeated independently three

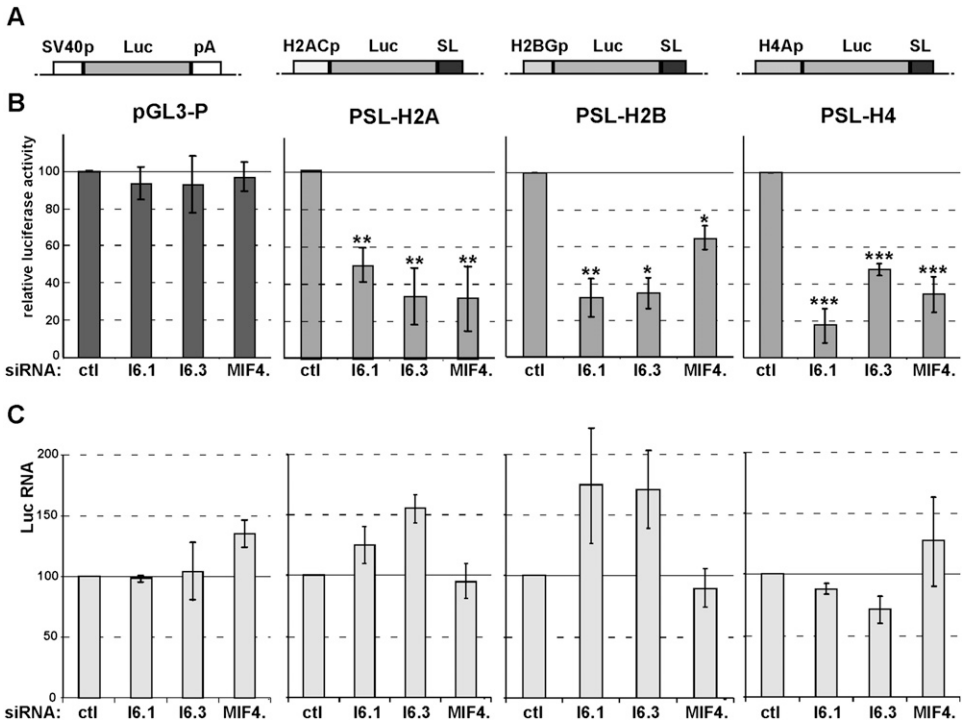

FIGURE 4. INT6 and MIF4GD requirement for efficient translation of mRNA ending with the histone stem–loop regulatory element. (*A*) Schematic representation of the four reporter constructs including the firefly luciferase coding sequence under control of an SV40 promoter and a poly(A) signal (pGL3-P) or under control of the promoter and stem–loop elements of the following human histone genes: *HIST1H2AC* (PSL H2A), *HIST1H2BG* (PSL-H2B), and *HIST2H4A* (PSL-H4). (*B*) After treatment with control, I6.1, I6.3, or *MIF4GD* siRNA duplexes, HeLa cells were transfected with these different constructs together with a *Renilla* luciferase expression vector to normalize transfection efficiency. Firefly and *Renilla* activities were measured in protein extracts of these cells using the dual luciferase assay. The graphs represent the means of the ratio with respect to the control siRNA condition of three independent experiments for the various siRNAs and reporter constructs as indicated. The error bar corresponds to the standard deviation, and stars are indicative of the results of the Student's *t*-test as described in the legend to Figure 2. (*C*) In these experiments, part of the transfected cells were kept aside to quantify the firefly and *Renilla* luciferase mRNA by RT-QPCR. The graphs represent the ratio of firefly luciferase mRNA amounts with respect to the control siRNA condition after normalization with *Renilla* luciferase mRNA for the various reporter constructs and RNA.

times, and the mean of the normalized firefly luciferase activity is represented (Fig. 4B). When the experiment was performed with a control vector including the firefly luciferase under the control of the SV40 promoter and poly(A) elements, there was no effect of INT6 and MIF4GD silencing on luciferase expression (Fig. 4B, pGL3-P panel). For all three constructs including firefly luciferase under histone gene promoters and 3′-end processing elements, a 60%–80% reduction was observed when cells were silenced for INT6 or MIF4GD expression. The effect obtained with the two INT6 siRNA duplexes was similar and comparable to that resulting from MIF4GD silencing (Fig. 4B, panels PSL-H2A, PSL-H2B, and PSL-H4). For this experiment, it was also checked that the observed effect was not due to a decrease in the mRNA amounts. To this end, total RNA was prepared from the transfected cells and analyzed by RT-qPCR for firefly and *Renilla* luciferase mRNAs. The INT6 silencing was not observed to reduce the firefly luciferase mRNA and even to slightly increase it in the case of the PSL-H2A and PSL-H2B constructs (Fig. 4C). This approach confirmed that, similarly to MIF4GD, INT6 silencing reduces translation of mRNA placed under the control of histone gene regulatory elements. Because this effect was observed using various siRNA duplexes directed against *INT6* mRNA, the possibility of an off-target effect was unlikely. To further test this point, a rescue analysis was done with the PSL-H4 construct. This plasmid was transfected in cells silenced either with a control or the I6.4 siRNA duplex. This latter one targets the 3′-untranslated region (3′ UTR) of the *INT6* mRNA. In such INT6-silenced cells, the protein was expressed from a vector lacking the 3′ UTR. As observed above, silencing of INT6 reduced firefly luciferase production, but expression of INT6 reverted this effect (Fig. 5A). Immunoblot analysis of INT6 and β-actin as loading control showed that these effects were correlated with lower and higher amounts of INT6 (Fig. 5B). A similar observation was done using the PSL-H2B construct (Fig. 5C), but with this construct, overexpression of INT6 was not able to raise expression significantly above the level observed with the control siRNAs. It was also tested whether overexpression of an INT6 mutant lacking the PCI domain had an inhibitory

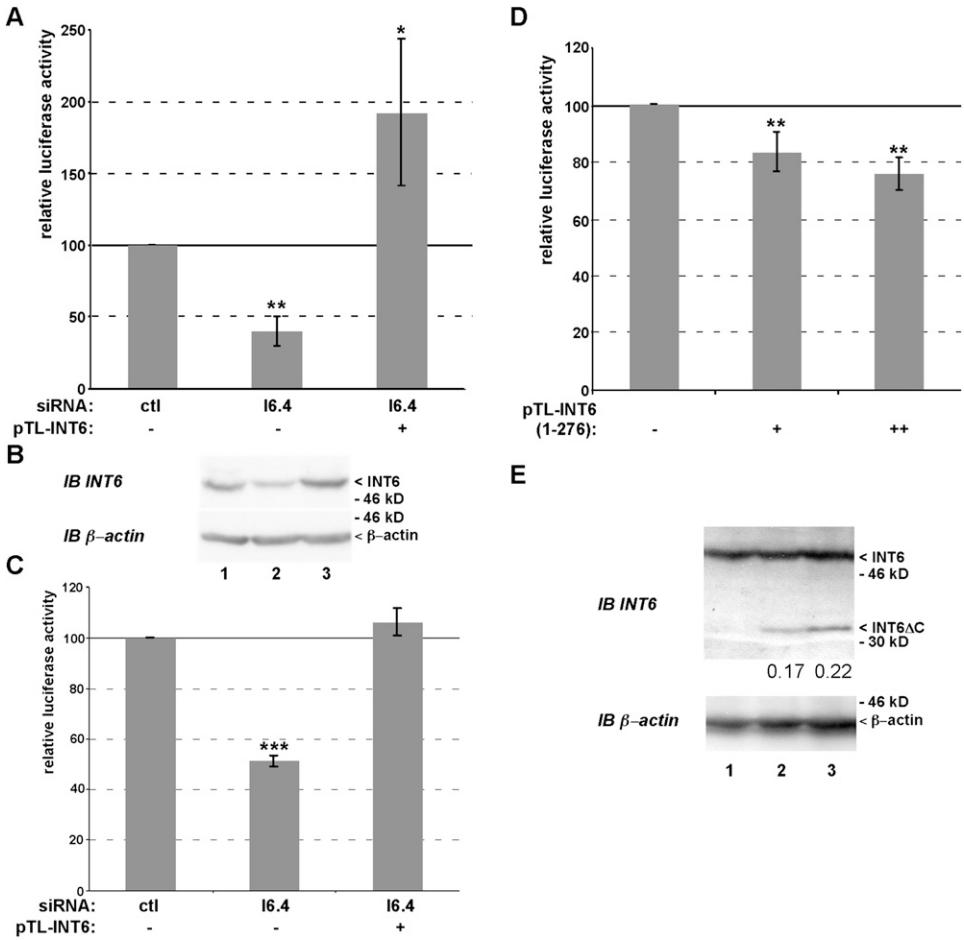

FIGURE 5. (*A*) Rescue of INT6 siRNA effect by expression of a resistant form of INT6. The experiment was performed as described in the legend to Figure 4 with the PSL-H4 reporter construct and the control or I6.4 siRNA duplexes. The latter matches with a sequence of the 3′ UTR of the *INT6* mRNA. Together with the luciferase constructs, cells were also cotransfected with a control or an INT6 expression vector lacking the 3′ UTR. Luciferase activity was measured and is represented as described in the legend to Figure 4. (*B*) Extracts of cells used for the experiment shown in panel *A* were analyzed by immunoblot using an antibody to INT6 (*top* panel) or to β-actin (*bottom* panel). The position of the signal corresponding to these proteins is indicated. (*C*) The experiment described in panel *A* was also performed with the PSL-H2B reporter construct. Results are represented as in *A*. (*D*) Inhibitory effect of overexpression of a C-terminally truncated INT6 mutant on PSL-H4 activity. 0.3×10^5 HeLa cells were transfected with the PSL-H4 reporter together with either an empty vector or 4 μg and 8 μg of a construct expressing an INT6 mutant corresponding to the N-terminal 276 amino acids. Luciferase activity was measured and is represented as described in the legend to Figure 4. (*E*) Extracts of cells used for the experiment shown in panel *C* were analyzed by immunoblot using an antibody directed against the N-terminal 19 amino acids of INT6 (*top* panel) or to β-actin (*bottom* panel). The position of the signal corresponding to INT6, INT6ΔC, and β-actin is indicated. The signals corresponding to INT6 and INT6ΔC were quantified, and numbers *below* the blot are the fractions of INT6ΔC with respect to INT6.

effect on histone gene expression by competing with the wild-type protein. To this end, cells were transfected with the PSL-H4 construct together with a control vector or increasing amounts of a construct expressing a protein corresponding to the N-terminal 276 amino acids of INT6. Expression of this INT6 mutant was observed to reduce the activity of the PSL-H4 reporter in a dose-dependent manner (Fig. 5D). The effect was limited, but the amount of overexpressed mutant was weak as compared with that of endogenous INT6 representing only 22% of the wild-type endogenous INT6 at the maximum (Fig. 5E). These observations confirmed that the effect on translation of histone mRNAs was due to the absence of INT6 and also showed that a mutant of this protein can exert a dominant-negative effect on this process. These various observations establish INT6 as an important protein for translation of canonical histones.

Interaction of INT6 with SLBP

Considering the interaction of INT6 with MIF4GD and knowing that this latter protein binds SLBP, we examined the association of INT6 with SLBP. This was first analyzed by performing an immunoprecipitation experiment from the endogenous proteins. A clear SLBP signal was detected in the INT6 immunoprecipitate (Fig. 6A, lane 3) and not when the antibody to INT6 was omitted in the reaction or when preimmune serum was used (Fig. 6A, lanes 1,2). We

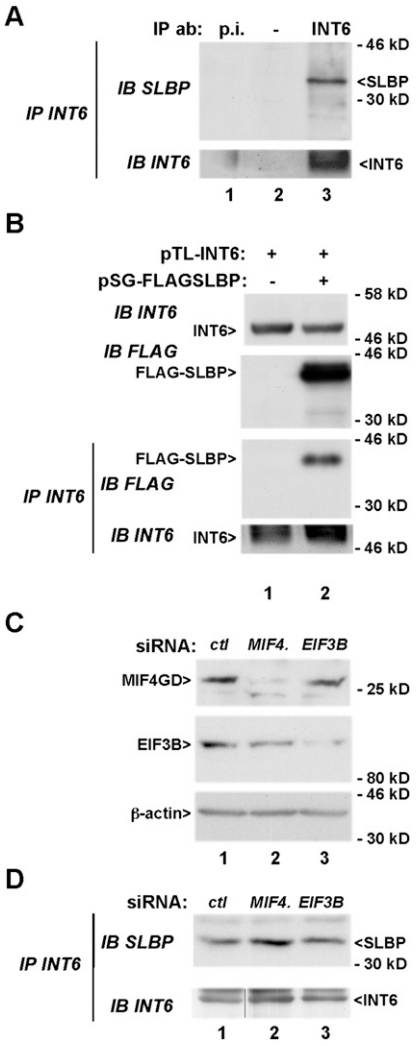

FIGURE 6. INT6 interacts with SLBP. (*A*) Extracts of HeLa cells were used for immunoprecipitation experiments performed with pre-immune serum (p.i., lane *1*), protein A-Sepharose beads only (lane *2*), and the C-20 antibody to INT6 (lane *3*). Immunoprecipitates were analyzed by immunoblot using a monoclonal antibody directed against SLBP (*top* panel) and an antibody to INT6 (*bottom* panel). Positions of the SLBP and INT6 signals are indicated on the *right* of the gel together with the position of bands of a molecular weight marker run in parallel. (*B*) HeLa cells were transfected with the pTL-INT6 (lanes *1* and *2*) and pSG-FLAGSLBP (lane *2*) expression vectors. Lysates from these transfected cells were analyzed by immunoblot using an antibody to INT6 (*top* panel) and to Flag (second panel from *top*). With these cell extracts, immunoprecipitation was performed using the antibody to INT6 (C20) in the presence of RNAse A, and the immunoprecipitates were analyzed by immunoblot with the monoclonal antibody to Flag (third panel from *top*) and to INT6 (*bottom* panel). The position of FLAGSLBP is indicated. (*C*) HeLa cells were transfected with control (lane *1*), *MIF4GD* (lane *2*), or *EIF3B* (lane *3*) siRNAs. Extracts of these cells were analyzed with antibodies to MIF4GD (*top* panel), to EIF3B (*middle* panel), and to β-actin (*bottom* panel). (*D*) These extracts were used for immunoprecipitation experiments performed using the C-20 antibody to INT6, and immunoprecipitates were analyzed with the antibody directed to SLBP (*top* panel) as in *A* and with the antibody to INT6 (*bottom* panel).

analyzed further if association between both proteins was RNA-dependent. HeLa cells were transfected with vectors expressing INT6 and SLBP tagged at its N terminus with a Flag epitope. Immunoprecipitation of INT6 in the presence of RNAse A coprecipitated FLAG-SLBP (Fig. 6B, bottom middle panel, lane 2). This experiment showed that RNA was not required for the association of both factors. A possibility was that MIF4GD bridges SLBP and INT6 by interacting with both proteins. To test this, the INT6–SLBP coimmunoprecipitation was analyzed using extracts of MIF4GD-silenced cells. The removal of MIF4GD, which was effective in the extract (Fig. 6C, top panel, cf. lanes 1 and 2), did not impair the association of INT6 with SLBP (Fig. 6D, top panel, cf. lanes 1 and 2). The SLBP signal was even slightly higher, but this was related to a higher efficiency of INT6 immunoprecipitation (Fig. 6D, bottom panel, cf. lanes 1 and 2). From these data, it appears that INT6 is able to interact with SLBP independently of MIF4GD. Because it was previously shown that SLBP interacts with eIF3, we further tested if perturbation of this complex affects the INT6 SLBP interaction (Ling et al. 2002; Gorgoni et al. 2005). As for MIF4GD, silencing of EIF3B, which is a core subunit of eIF3 essential for translational activity, did not reduce coimmunoprecipitation of INT6 and SLBP (Fig. 6C, middle panel, lane 3; Fig. 6D, top panel, cf. lanes 1 and 3). Collectively, these results indicate that there is a specific association of INT6 with SLBP, which does not require MIF4GD or an eIF3 core subunit like EIF3B. This suggests that MIF4GD is likely recruited by both INT6 and SLBP and that its functional effect on translation might depend on association with additional translation initiation factors other than eIF3.

Colocalization of INT6 and MIF4GD in the cytoplasm

To ascertain that INT6 and MIF4GD interact in the cellular context, we performed immunofluorescence studies. It was first checked that the MIF4GD subcellular localization analyzed with the rabbit polyclonal antibody that we developed is similar to that detected by expressing MIF4GD fused to the HA epitope with the antibody to HA. Immunostaining with the antibody raised against the N-terminal first 20 amino acids of MIF4GD showed a weak nuclear punctate pattern with more intense cytoplasmic dots (Supplemental Fig. S3A, panel a). Analysis with the monoclonal antibody to HA showed a similar pattern with a clear colocalization of the cytoplasmic dots detected with both antibodies (Supplemental Fig. S3A, panels c and e). We concluded from these observations that MIF4GD is mainly localized in the cytoplasm in which it forms foci where the protein is concentrated. It was next tested how this localization compares with that of SLBP. Subcellular localization of both endogenous proteins was analyzed using the antibody to MIF4GD that we developed, along with a mouse monoclonal antibody directed against SLBP. Both proteins were

mainly detected in the cytoplasm, where they form a punctate pattern (Supplemental Fig. S3B), and were clearly colocalized in some dots, but not in all. Indeed, some MIF4GD foci were not stained by the SLBP antibody (Supplemental Fig. S3B, panel e). This indicates a partial cytoplasmic colocalization of SLBP and MIF4GD. We then compared the subcellular localization of MIF4GD and INT6. When cells were transfected with vectors expressing the INT6FLAG and MIF4GDHA fusion proteins and analyzed with the rabbit polyclonal antibody to INT6 along with the mouse monoclonal antibody to HA, INT6 was detected both in the nucleus and the cytoplasm, where it formed dots that showed a very good colocalization with those formed by MIF4GD (Fig. 7a–e). A very similar pattern was observed by transfecting the cells solely with the MIF4GDHA expression vector and staining the endogenous INT6 with the C-169 rabbit antibody to INT6 and MIF4GDHA with the monoclonal antibody to HA (Fig. 7f–j). The patterns observed for endogenous INT6 without (Supplemental Fig. S3C) or with coexpression of MIF4GDHA were similar. Finally, this pattern with nuclear and cytoplasmic INT6 along with INT6-MIF4GD colocalization in cytoplasmic dots was also observed by transfecting cells solely with the INT6FLAG expression vector and by revealing the proteins with the monoclonal antibody to Flag and the rabbit polyclonal antibody to MIF4GD (Fig. 7k–o). These observations are in agreement with the notion that MIF4GD binds INT6 and indicated that MIF4GD is mainly present in the cytoplasm, whereas INT6 can be detected in both nucleus and cytoplasm. They also showed that both proteins are colocalized in cytoplasmic foci in which SLBP can be observed, in agreement with all three factors participating in histone mRNA translation.

DISCUSSION

INT6 as an eIF3 subunit necessary for histone mRNA translation

INT6 has been identified in numerous organisms from fission yeast to human and is highly conserved (Marchetti et al. 1995; Desbois et al. 1996; Morris-Desbois et al. 1999; Bandyopadhyay et al. 2000; Crane et al. 2000). It has also been characterized as one of the 13 subunits composing the 800-kDa eIF3 complex (Asano et al. 1997), but its activity in this important translation initiation complex remains to be understood in detail, especially because some discrepancies can be considered by comparing results from

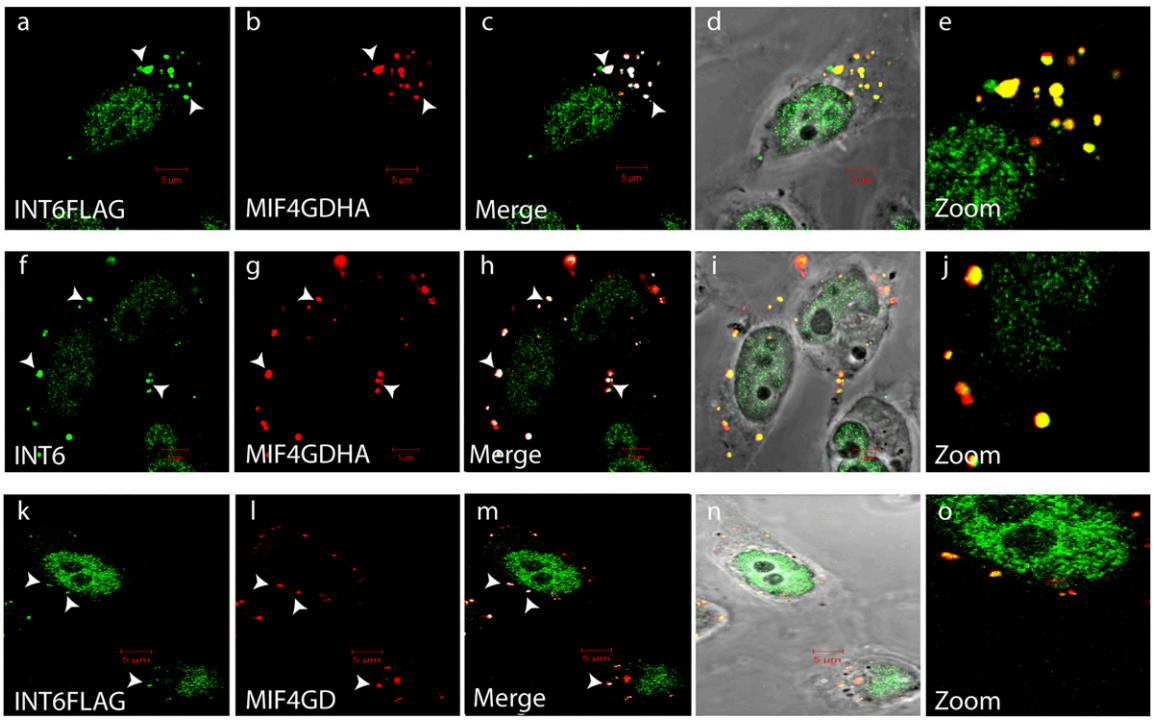

FIGURE 7. Colocalization in the cytoplasm of INT6 and MIF4GD. HeLa cells were transfected with the MIF4GDHA and INT6FLAG expression vectors in combination (panels *a–e*), with only the former (panels *f–j*), or with only the latter (panels *k–o*). The cells were stained with the following combination of antibodies: C-169 antibody to INT6 and monoclonal antibody to HA (panels *a–j*), monoclonal antibody to Flag and rabbit antiserum to MIF4GD (panels *k–o*). Representative confocal images are shown, as well as superimpositions of both stainings (panels *c,h,m*) and of the stainings with the corresponding transmission image (panels *d,i,n*). In panels *c*, *h*, and *m*, colocalization was evaluated by using the Colocalization Highlighter plug-in of ImageJ software; colocalized pixels appear in white. (White arrows) Examples of cytoplasmic foci with colocalization of INT6 and MIF4GD. An enlargement of the picture corresponding to colocalizing foci is also shown (panels *e,j,o*). Scale bars, 5 μm.

different in vitro and in vivo studies. Mass spectrometry analyses have shown that each of the 13 eIF3 subunits is present at one copy, and three different subcomplexes have been observed by favoring dissociation in response to increased ionic strength (Zhou et al. 2008). One includes the a, b, c, i, and g subunits, which correspond to the five core subunits of the *Saccharomyces cerevisiae* eIF3 complex (Asano et al. 1998; Phan et al. 1998). Another subcomplex consists of the f, h, and m subunits and the third subcomplex to the k, l, e, d, and c subunits. Association of this latter with the other subunits is likely to depend on the c subunit with which INT6 interacts (Morris-Desbois et al. 1999). In the eIF3 complex, some subunits are essential, probably mainly the a, b, and c subunits, but others are likely to play a role in the translation of specific mRNAs or to allow specific regulations. Despite characterization of an interaction of INT6 with eIF4G (LeFebvre et al. 2006) and its requirement for reconstitution from baculovirus-expressed subunits of a minimal complex allowing binding of the 48S on the initiation codon (Masutani et al. 2007), several studies have ruled out a role of the protein for bulk translation (Bandyopadhyay et al. 2000; Zhou et al. 2005; Grzmil et al. 2010). Indeed, it has been reported that deletion of the gene in fission yeast does not affect general translation or a polysome profile (Zhou et al. 2005). However, in this organism, it has been observed that eIF3e was necessary for stability of the complex when yeast were grown in minimal medium (Akiyoshi et al. 2001). Also in human cells, suppression of INT6 by RNA interference does not affect bulk translation and a polysome profile (Grzmil et al. 2010). However, it has been reported that INT6 was important for translation of specific genes. Grzmil et al. (2010) have observed that in the MDA-MB-231 breast cancer cell line, INT6 was able to act positively or negatively on the presence of several mRNAs in polysomes. In the same line, Zhou et al. (2005) observed the existence of two eIF3 complexes in fission yeast, one including eIF3e and the other eIF3m, each type of complex associating with different mRNA subsets. The data presented in this study identify the genes encoding the canonical histones as a new class of genes in which translation depends on INT6/EIF3E.

Activity of INT6 in histone mRNA translation involves interaction with MIF4GD and SLBP

A specific feature of histone mRNAs is to lack a poly(A) tail and to include a particular stem–loop motif at their 3′ end. This structure binds the SLBP protein, which plays a key role in 3′ processing (Dominski and Marzluff 2007), nuclear export (Ghule et al. 2008; Sullivan et al. 2009a), and translation (Ling et al. 2002; Gorgoni et al. 2005) of these mRNAs during the S phase. The effect of SLBP on translation has been shown to involve eIF3 and eIF4G. More recently, Cakmakci et al. (2008) have also shown that this effect on translation involves an interaction of SLBP with MIF4GD/SLIP1, which was characterized in a two-hybrid screen with SLBP as bait. Similarly, we obtained a clone including the entire MIF4GD coding sequence in a two-hybrid screen using INT6 as bait. In agreement with this interaction, we observed that INT6 is also an essential protein for efficient translation of the histone genes. This was observed using the RNA interference approach on endogenous histone genes, but also with heterologous constructs including the luciferase reporter gene under the control of the histone promoter and stem–loop regulatory elements. The effect observed by silencing INT6 was of similar magnitude as compared with suppression of MIF4GD or SLBP (Cakmakci et al. 2008; J Neusiedler, unpubl.). Thus, if INT6 is dispensable for the translation of the majority of cellular genes, it plays an essential role for histone mRNAs. The interaction with MIF4GD is likely part of this effect. However, the possibility of a direct binding of INT6 to SLBP exists, although this aspect will require further investigation. Indeed, immunoprecipitation experiments showed a clear SLBP signal when INT6 was precipitated, and the association was not dependent on MIF4GD or EIF3B. Previous biochemical studies have shown the essential role of this core subunit in the assembly of the eIF3 complex (Asano et al. 1998; Phan et al. 1998; Masutani et al. 2007; Zhou et al. 2008). However, it remains possible that the association between SLBP and EIF3E involves other eIF3 subunits, possibly those that form a subcomplex with EIF3E as c, k, l, and d. It is likely that the SLBP–eIF3 association involves several contacts including those with MIF4GD that probably have a stabilizing effect.

Interestingly, INT6 appears to interact with several proteins including a MIF4G domain. Indeed, we have previously shown that it binds UPF2, which includes three MIF4G domains, as well as CBP80, which also includes one (Morris et al. 2007). Finally, we show here that the small MIF4GD protein that mainly corresponds to a MIF4G domain binds INT6. Hence, INT6 is likely to interact specifically with the MIF4G domain, and as shown here, this ability relies on the N-terminal two-thirds of the protein, but does not necessitate the C-terminal PCI domain, which probably has a scaffold role permitting association with the other eIF3 subunits. LeFebvre et al. (2006) have described an in vitro interaction between the 1015–1118 region of eIF4G and the eIF3 complex that would involve a contact with INT6 as observed by performing partial proteolysis and mass spectrometry analyses. Thus it is possible that INT6 interacts simultaneously with both MIF4GD and eIF4G, thereby playing a pivotal role. Both interactions would involve the N-terminal two-thirds of INT6 (LeFebvre et al. 2006). For poly(A)–tailed mRNAs, the looping of the molecule through contacts of poly(A)–bound proteins with eIF3 and eIF4G has been shown to be important for efficient translation initiation (Amrani et al. 2008; Martineau et al. 2008). In mammalian cells, PABP does not directly contact eIF3, and this involves PAIP1. Martineau et al. (2008)

have shown an interaction of PAIP1 mainly with EIF3G. However in a far-western experiment, they also revealed bands migrating at the position of EIF3E, and they show in this study that the stimulatory effect of PAIP1 overexpression is lost when INT6 is silenced. Interestingly, PAIP1 also includes an MIF4G domain. Hence, although the 3′ end of the histone gene lacks a poly(A) tail, the general mRNP organization allowing efficient translation initiation might be very similar, with SLBP–MIF4GD acting in a similar way as PABP–PAIP1 by allowing looping of the RNA along with contacts with eIF4G and eIF3. For the majority of mRNAs, the absence of INT6 might be made up for by other contacts, possibly with EIF3G in particular (Martineau et al. 2008), whereas for histone mRNAs, the absence of EIF3E appears detrimental.

Relationship between histone mRNA translation and other roles of INT6

Previous studies of INT6 function have led to several observations that are likely related to its role in histone mRNA translation. In particular, it has been reported that INT6 is partly located in the nucleus (Desbois et al. 1996; Morris-Desbois et al. 1999; Buchsbaum et al. 2007; Grzmil et al. 2010), and Watkins and Norbury (2004) have shown that in nontransformed cells this localization was reduced in S phase. In agreement with a dual location in the nucleus and the cytoplasm, the protein has an N-terminal nuclear export sequence and an internal nuclear localization signal, indicating that it is likely to shuttle between both compartments (Guo and Sen 2000). Mutation of the NES renders the protein exclusively nuclear. In addition, it has been observed that INT6 can be associated with the RNA polymerase II holoenzyme (J-M Egly and P Jalinot, unpubl.). Considering the interaction with SLBP that lacks an NES, these observations raise the possibility that INT6 might be loaded on histone mRNAs cotranscriptionally and thereby might participate in their export toward the cytoplasm. SLBP has been shown previously to play an important role in this process (Ghule et al. 2008; Sullivan et al. 2009a). This nuclear presence of INT6 is specific because other subunits of eIF3 are exclusively cytoplasmic (Watkins and Norbury 2004). In the cytoplasm, it is possible that, by interacting with other subunits of the eIF3 complex, INT6 favors assembly of the complete eIF3 on histone mRNAs as well as establishment of the various interactions with other general translation initiation factors. Alternatively, in the cytoplasm, INT6 associated to SLBP might be replaced by a complete eIF3 complex. To test these notions, it will be interesting to analyze in detail the dynamics of the recruitment of the various eIF3 subunits to this particular type of mRNA and to verify that the nuclear presence of INT6 is, indeed, important to their translation.

In addition, it is possible that INT6 intervenes at further steps of histone mRNA metabolism. Indeed, once genome replication is completed, histone expression stops, and their mRNAs are degraded in a process that involves UPF1, a core NMD factor (Kaygun and Marzluff 2005). Intriguingly, we have previously shown that INT6 was important for the NMD process and was able to interact with UPF2 and UPF1 (Morris et al. 2007). Hence, it might be possible that after playing a positive role in S phase, INT6 also participates in histone mRNA degradation in G_2. To better understand this point, it will be important to determine the exact role played by UPF1 and RNA degradation factors in the process and also to identify what could make INT6 switch from a positive to a negative role.

Another activity of INT6 that might be related to its role in histone mRNA translation is the control it exerts on the stability of the MCM7 subunit of the MCM complex, which is a key factor of DNA replication initiation and progression (Buchsbaum et al. 2007). Indeed, we have previously shown that in S phase INT6 binds polyubiquitinylated MCM7 and protects it from degradation by the proteasome. In this study, silencing of both INT6 and MCM7 was observed to impede normal DNA replication (Buchsbaum et al. 2007). By considering these two sets of data, it is possible that INT6 acts as a sensor of DNA replication progression and allows coupling of this process with histone expression. One possibility would be that the INT6 chromatin-bound fraction by interacting with polyubiquitinylated MCM7 cannot favor histone mRNA maturation and translation, thereby establishing a negative feedback loop allowing adjustment of histone production and DNA replication completion. Future studies should help to establish the validity of such a model and to determine precisely if both activities are independent or related.

In conclusion, our observations have established an important role of INT6 for translation of the mRNAs encoding canonical histones and thereby open new perspectives to understand how several activities of this protein might be related. They also might bring some interesting new ideas on the mechanisms allowing coupling of DNA replication and histone synthesis. Finally, this activity by influencing genomic stability is certainly important to consider for gaining a better understanding of the oncogenic and genomic instability effects resulting from INT6 alteration (Marchetti et al. 1995; Yen and Chang 2000; Rasmussen et al. 2001; Morris and Jalinot 2005; Mack et al. 2007).

MATERIALS AND METHODS

Two-hybrid assay

A two-hybrid screen of a cDNA library of human lymphocytes immortalized by EBV (Durfee et al. 1993) with INT6 fused to the DNA binding domain of GAL4 was performed as previously described (Morris-Desbois et al. 1999). Three cDNA clones encoding MIF4GD were isolated and sequenced: THI 22 (full coding sequence amino acids 1–222), THI 2, and 21 (amino acids 17–222).

Constructs

Expression vectors for MIF4GD (NM-020679.2) alone or fused at its C-terminal end with the HA epitope were generated by PCR amplification from the SC113046 clone (OriGene Technologies) with the 5′ primer 5′-AGGAATTCTGGCTAGTCATGGGGGAGCCCAG TAGAGAG-3′ and as 3′ primer either 5′-TCTGGAGATCTAGTCGG AGACTTCGCTGTAG-3′ or 5′-GTAGAAGATCTCGAGCTAGGC GTAGTCAGGCACGTCGTAGGGATACCCGTCGGAGACTTCGCT GTAG-3′ (HA fusion). The amplified fragments were digested by EcoRI and BglII restriction enzymes and inserted between the EcoRI and BglII sites of the pTL1 expression vector (pSG5 derivative) (Green et al. 1988). The pTL-INT6(1–276) expression vector was generated by digesting pTL-INT6 by BglII and XhoI. The extremities were filled in, and the vector was ligated. This vector expresses the N-terminal 276 amino acids of INT6 with the addition of an RSY motif at the C terminus. The constructs including the firefly luciferase under the control of the promoter and stem–loop elements of histone genes were constructed in two steps. First, a sequence including the stem–loop and histone downstream element was amplified from total DNA prepared from Jurkat cells for the *HIST1H2AC*, *HISTH2BG*, and *HIST2H4A* genes with the following primers:

H2ACSL5′: 5′-GTGATTCTAGAGGTATCTGAGCTCCCGGAAAC-3′;
H2ACSL3′: 5′-TCCCCAGGATCCGAAAAGCAGTAATACGCTTTG-3′;
H2BGSL5′: 5′-GTAAATCTAGACTTAGGTGCTTTAAAACTCAAA GG-3′;
H2BGSL3′: 5′-CCACGGGATCCAAACTGGTCTCGATCCGCACG CC-3′;
H4ASL5′: 5′-GGCCGCCTCTAGAGCTTTGCACGTTTCGATCCC-3′;
H4ASL3′: 5′-ACTTCGGATCCGATTGTCGCCCCACTGCCAAAG-3′.

The amplified fragments were digested with the XbaI and BamHI restriction enzymes and inserted between the XbaI and BamHI restriction sites of the pGL3 promoter (Promega). The promoter sequences of these histone genes were similarly amplified from Jurkat cell DNA using the following primers:

H2ACP5′: 5′-GTAAAGATCTGATTTCTGCTACTTATAGGG-3′;
H2ACP3′: 5′-TCCAGCCATGGCAATCAGACAAAAATCACC-3′;
H2BGP5′: 5′-ATCGGTAGATCTGTGAAAGGCGCAATTTGATTGG-3′;
H2BGP3′: 5′-GGTTCAGCCATGGTGTCAGAAAACAATAACAGC AG-3′;
H4AP5′: 5′-GCGTGTAGATCTCATCGTCGGAACGGCGCTTCC-3′;
H4AP3′: 5′-TGCCGGCCATGGCCGCTGGAGCCCGATAGACA GC-3′.

The amplified fragments were digested by the XhoI and NcoI restriction enzymes and inserted between the XhoI and NcoI sites of the pGL3-promoter derivatives containing the stem–loop sequences instead of the poly(A) signal giving expression vectors PSL-H2A, PSL-H2B, and PSL-H4. The various constructs used in this study were controlled by DNA sequencing.

Cell culture and transfection

HeLa cells were maintained in Dulbecco's Modified Eagle's Medium supplemented with 10% FCS (Invitrogen), 100 units/mL penicillin, and 100 μg/mL streptomycin at 37°C in a 5% CO_2-humidified atmosphere. For plasmids and siRNA transfections, the amount of FCS used in the culture medium was reduced to 5%, and antibiotics were omitted for siRNA transfection, which was performed using the Lipofectamine 2000 reagent according to the manufacturer's instructions (Invitrogen). siRNA duplexes I6.1, I6.3, I6.4, and anti-EIF3B have been described previously (Morris and Jalinot 2005; Morris et al. 2007). For endogenous histone labeling experiments, a *Luc* siRNA duplex was used. For experiments with luciferase constructs, the control siRNA was a scrambled sequence of I6.1 (5′-GACGUGCCAGGAUGAUUGG dTdT-3′). For *MIF4GD* mRNA, the sequence of the siRNA duplex on the sense strand was 5′-CCAGUAGAGAGGAGUAU AAdTdT-3′. For DNA and siRNA transfection, HeLa cells were first transfected with the siRNAs using Lipofectamine 2000, and 24 h later, the cell culture medium was changed and transfection of DNA vectors was performed with the calcium phosphate procedure. After 16 h, the culture medium was changed after a PBS wash, and the cells were harvested 48 h later.

Metabolic pulse-labeling of cellular proteins

HeLa cells were transfected with the various siRNA duplexes as described above. For G_1/S synchronization, 24 h after siRNA transfection 2.5 mM thymidine (Sigma-Aldrich) was added to the medium for 18 h, then removed for 10 h and added again at the same concentration for 14 h. Cells were then released from the double-thymidine block and incubated in DMEM for 1.5 h. They were further cultured in DMEM lacking methionine for 30 min. Cells were then incubated in DMEM supplemented with ^{35}S-labeled methionine and cysteine for 10 min. Cells were collected and histones were prepared from isolated nuclei by acidic extraction as previously described (Cakmakci et al. 2008). The histone fraction was analyzed by SDS-PAGE on 16% polyacrylamide gels that were first stained with Coomassie Blue and further analyzed for radioactivity using a Fuji phosphorimager (Fujifilm). Radioactivity in the bands corresponding to histones was quantitated using the Fuji ImageGauge software using the profile mode.

Immunoprecipitation and immunoblot

For immunoprecipitation, extracts of HeLa cells were prepared in RIPA buffer (Harlow and Lane 1988) supplemented with TCEP (10 mM) and Pefabloc and Complete protease inhibitors (Roche). The immunoprecipitations of Figures 1B and 6B were performed with the same buffer but without sodium dodecyl sulfate. Lysates were centrifuged for 15 min at 14,000 rpm, and the protein concentration of supernatants was measured with the DC Protein Assay kit (Bio-Rad). After adjustment to equal protein concentrations, 5% of these extracts were analyzed by immunoblot to monitor protein expression. Immunoprecipitation was performed by overnight incubation with antibodies diluted 1:250, and protein A-Sepharose beads equilibrated in RIPA buffer were further added. After incubation for 1.5 h, beads were collected by centrifugation and washed three times in RIPA buffer. When indicated, incubation with the antibody was done at room temperature in the presence of 20 μg of RNAse A for 300 μL of extract. Proteins were eluted in 4× SDS sample buffer for 10 min at 92°C. After separation by SDS-PAGE, proteins were transferred to a polyvinylidene difluoride (PVDF) membrane (GE Healthcare Life Sciences). For immunoblot, primary antibodies were diluted 1:1000 or at the concentration indicated by the manufacturer.

Detection was performed by chemiluminescence using the ECL or ECL plus reagent (GE Healthcare Life Sciences) using secondary antibodies diluted 1:6000 or 1:10,000, respectively.

Immunofluorescence and confocal microscopy

Immunofluorescence was performed as previously described using 5×10^4 HeLa cells (Morris-Desbois et al. 1999). Briefly, cells were fixed for 20 min with 4% paraformaldehyde and further washed three times with PBS. Free aldehydic groups were blocked by incubation with 0.1 M glycine for 15 min. For permeabilization, cells were incubated for 5 min in 1 mL of 0.1% PBS-Triton X-100 and further incubated with 1% BSA at room temperature (15–30 min). Cells were washed three times with PBS, and the primary antibody was incubated for 1.5 h at room temperature; cells were further washed three times with PBS. The secondary antibody conjugated with Alexa Fluor 488 or Alexa Fluor 546 (Invitrogen) was then incubated for 1 h in the dark, and the cells were further washed three times with PBS and once with distilled water. Finally, cells were mounted in Vectashield DAPI (1.5 μg/mL; Vector Laboratories). Slides were observed with an Axioplan 2 LSM 510 upright confocal microscope (Carl Zeiss AG). Colocalization was evaluated either by visual inspection of signal overlap on merged images (Supplemental Fig. S3) or by using the Colocalization Highlighter plug-in of ImageJ software (National Institutes of Health) (Fig. 7). Threshold settings for each image were automatically set with the threshold tool and assigned to the input window of the Colocalization Highlighter plug-in. The ratio of intensity was set at 50%. Two points are considered as colocalized if their respective intensities are higher than the threshold of their channels and if their ratio of intensity is higher than 50%.

Antibodies

The antibodies used in this study were as follows: INT6 C-169 rabbit antiserum (Morris-Desbois et al. 1999), mouse monoclonal antibodies to Flag (clone M2; Sigma-Aldrich) and to HA (clone 7; Sigma-Aldrich), goat polyclonal antibody to EIF3B (A-20; Santa Cruz Biotechnology), and mouse monoclonal antibody to SLBP (clone 2C4-1C8; Novus Biologicals). The antibody directed against MIF4GD was obtained by immunizing a rabbit with a peptide corresponding to the first N-terminal 20 amino acids of the protein coupled to ovalbumin.

Northern blot and nCounter RNA analysis

Total RNAs (20 μg) purified using the Total RNA Isolation Kit (Macherey-Nagel) were separated on a 8% polyacrylamide/7 M urea gel. Their integrity was verified by ethidium bromide staining of the gel, and they were further transferred by capillarity to a Hybond-N^+ membrane (GE Healthcare Biosciences). The probes (H2B: 5′-GTGTACTTGGTGACGGCCTT-3′; H3: 5′-GCCTCCTGCAGCG CCATCAC-3′; H4: 5′-GTCTTGCGCTTGGCGTGCTC-3′) were radiolabeled with [γ-^{32}P]ATP using T4 polynucleotide kinase (New England Biolabs) and hybridized to the membrane in hybridization buffer (5× SSC, 20 mM Na_2HPO_4 at pH 7.2, 7% SDS, 2× Denhardt's Solution, 50 μg/mL denatured salmon sperm DNA) for 16 h at 37°C. The membrane was then washed with stringent wash buffer (1× SSC, 1% SDS) and submitted to autoradiography using a phosphorimager.

For nCounter RNA analysis, two sequence-specific probes for each transcript were designed by the NanoString company. The capture probe was complementary to an ~50-base region of the mRNA plus a short common sequence coupled to biotin. The adjacent reporter probe was complementary to a second ~50-base region of the transcript and was coupled to a digital fluorescent reporter composed of a unique combination of four spectrally nonoverlapping dyes. These probes were designed for all of the main genes encoding canonical or variant histones with the exception of those exhibiting a very low or highly tissue-specific expression as inferred from the data given by the EST profile viewer of the Unigene resource (Boguski and Schuler 1995) of the National Center for Biotechnology Information. The probes, which were designed not to cross-hybridize with other histone mRNAs, were generally located in the divergent sequences located at the 3′ end upstream of the stem–loop. To the list of 30 histone genes were added *EIF3E* and *MIFG4GD*, as well as a group of six genes (*CSNK2B*, *ENO1*, *GAPDH*, *GNB2L1*, *RPL35A*, *TKT*, *YWHAQ*) that were selected on the basis of their weak expression variations in siRNA experiments performed in HeLa cells as evaluated by microarray analyses (P Descombes, pers. comm.). Direct measurement of the mRNA levels of these genes was performed using 100 ng of total RNAs with the nCounter apparatus (Geiss et al. 2008) according to the manufacturer's instructions. Counts for each transcript were analyzed using an Excel macro made at the Genomics Platform, Center Médical Universitaire, University of Geneva, Switzerland, for correction of background and normalization, as previously described (Beaume et al. 2011).

Real-time quantitative RT-PCR

Total RNAs were extracted using the Nucleic Acid and Protein Purification Kit (Macherey-Nagel). One-step RT-PCR reactions were performed using the QuantiTect SYBR Green RT-PCR kit (QIAGEN) and the LightCycler apparatus (Roche) according to the cycling conditions specified in the handbook of the kit. Gene-specific primers were designed using the Primer3 software. The sequence of the sense and antisense primers used for quantitative PCR was as follows: firefly luciferase: 5′-TCAAAGAGGCGAACT GTGTG-3′, 5′-GGTGTTGGAGCAAGATGGAT-3′; *Renilla* luciferase: 5′-TCGTCCATGCTGAGAGTGTC-3′, 5′-CTAACCTCGCC CTTCTCCTT-3′.

SUPPLEMENTAL MATERIAL

Supplemental material is available for this article.

ACKNOWLEDGMENTS

We are grateful to P. Descombes and D. Chollet of the University of Geneva Genomics Platform for performing the NanoString nCounter analyses. We also thank A. Roisin for help with cell culture. We acknowledge the contribution of the Genetic Analysis, Flux Cytometry and PLATIM platforms (S. Mouradian, C. Lionnet, and C. Chamot) of SFR Biosciences Gerland-Lyon Sud (UMS344/US8). This work was supported by a fellowship from Ligue Nationale contre le cancer (to J.N.) and by grants and fellowships (to J.N., V.M.) from Association pour la Recherche sur le Cancer.

Received February 2, 2012; accepted March 6, 2012.

REFERENCES

Akiyoshi Y, Clayton J, Phan L, Yamamoto M, Hinnebusch AG, Watanabe Y, Asano K. 2001. Fission yeast homolog of murine Int-6 protein, encoded by mouse mammary tumor virus integration site, is associated with the conserved core subunits of eukaryotic translation initiation factor 3. *J Biol Chem* **276:** 10056–10062.

Amrani N, Ghosh S, Mangus DA, Jacobson A. 2008. Translation factors promote the formation of two states of the closed-loop mRNP. *Nature* **453:** 1276–1280.

Asano K, Merrick WC, Hershey JW. 1997. The translation initiation factor eIF3-p48 subunit is encoded by *int-6*, a site of frequent integration by the mouse mammary tumor virus genome. *J Biol Chem* **272:** 23477–23480.

Asano K, Phan L, Anderson J, Hinnebusch AG. 1998. Complex formation by all five homologues of mammalian translation initiation factor 3 subunits from yeast *Saccharomyces cerevisiae*. *J Biol Chem* **273:** 18573–18585.

Bandyopadhyay A, Matsumoto T, Maitra U. 2000. Fission yeast Int6 is not essential for global translation initiation, but deletion of *int6*$^+$ causes hypersensitivity to caffeine and affects spore formation. *Mol Biol Cell* **11:** 4005–4018.

Beaume M, Hernandez D, Docquier M, Delucinge-Vivier C, Descombes P, Francois P. 2011. Orientation and expression of methicillin-resistant *Staphylococcus aureus* small RNAs by direct multiplexed measurements using the nCounter of NanoString technology. *J Microbiol Methods* **84:** 327–334.

Boguski MS, Schuler GD. 1995. ESTablishing a human transcript map. *Nat Genet* **10:** 369–371.

Buchsbaum S, Morris C, Bochard V, Jalinot P. 2007. Human INT6 interacts with MCM7 and regulates its stability during S phase of the cell cycle. *Oncogene* **26:** 5132–5144.

Cakmakci NG, Lerner RS, Wagner EJ, Zheng L, Marzluff WF. 2008. SLIP1, a factor required for activation of histone mRNA translation by the stem–loop binding protein. *Mol Cell Biol* **28:** 1182–1194.

Chen L, Uchida K, Endler A, Shibasaki F. 2007. Mammalian tumor suppressor Int6 specifically targets hypoxia inducible factor 2α for degradation by hypoxia- and pVHL-independent regulation. *J Biol Chem* **282:** 12707–12716.

Chen L, Endler A, Uchida K, Horiguchi S, Morizane Y, Iijima O, Toi M, Shibasaki F. 2010. Int6/eIF3e silencing promotes functional blood vessel outgrowth and enhances wound healing by upregulating hypoxia-induced factor 2α expression. *Circulation* **122:** 910–919.

Crane R, Craig R, Murray R, Dunand-Sauthier I, Humphrey T, Norbury C. 2000. A fission yeast homolog of Int-6, the mammalian oncoprotein and eIF3 subunit, induces drug resistance when overexpressed. *Mol Biol Cell* **11:** 3993–4003.

Desbois C, Rousset R, Bantignies F, Jalinot P. 1996. Exclusion of Int-6 from PML nuclear bodies by binding to the HTLV-I Tax oncoprotein. *Science* **273:** 951–953.

Dominski Z, Marzluff WF. 2007. Formation of the 3′ end of histone mRNA: Getting closer to the end. *Gene* **396:** 373–390.

Dominski Z, Yang XC, Marzluff WF. 2005. The polyadenylation factor CPSF-73 is involved in histone-pre-mRNA processing. *Cell* **123:** 37–48.

Durfee T, Becherer K, Chen P-L, Yeh S-H, Yang Y, Kilburn AE, Lee W-H, Elledge SJ. 1993. The retinoblastoma protein associates with the protein phosphatase type 1 catalytic subunit. *Genes Dev* **7:** 555–569.

Geiss GK, Bumgarner RE, Birditt B, Dahl T, Dowidar N, Dunaway DL, Fell HP, Ferree S, George RD, Grogan T, et al. 2008. Direct multiplexed measurement of gene expression with color-coded probe pairs. *Nat Biotechnol* **26:** 317–325.

Ghule PN, Dominski Z, Yang XC, Marzluff WF, Becker KA, Harper JW, Lian JB, Stein JL, van Wijnen AJ, Stein GS. 2008. Staged assembly of histone gene expression machinery at subnuclear foci in the abbreviated cell cycle of human embryonic stem cells. *Proc Natl Acad Sci* **105:** 16964–16969.

Gorgoni B, Andrews S, Schaller A, Schumperli D, Gray NK, Muller B. 2005. The stem–loop binding protein stimulates histone translation at an early step in the initiation pathway. *RNA* **11:** 1030–1042.

Green S, Issemann I, Sheer E. 1988. A versatile in vivo and in vitro eukaryotic expression vector for protein engineering. *Nucleic Acids Res* **16:** 369. doi: 10.1093/nar/16.1.369.

Grzmil M, Rzymski T, Milani M, Harris AL, Capper RG, Saunders NJ, Salhan A, Ragoussis J, Norbury CJ. 2010. An oncogenic role of eIF3e/INT6 in human breast cancer. *Oncogene* **29:** 4080–4089.

Guo J, Sen GC. 2000. Characterization of the interaction between the interferon-induced protein P56 and the Int6 protein encoded by a locus of insertion of the mouse mammary tumor virus. *J Virol* **74:** 1892–1899.

Harlow E, Lane D. 1988. *Antibodies: A laboratory manual*. Cold Spring Harbor Laboratory, Cold Spring Harbor, NY.

Hershey JW. 2010. Regulation of protein synthesis and the role of eIF3 in cancer. *Braz J Med Biol Res* **43:** 920–930.

Hinnebusch AG. 2006. eIF3: A versatile scaffold for translation initiation complexes. *Trends Biochem Sci* **31:** 553–562.

Hoareau Alves K, Bochard V, Rety S, Jalinot P. 2002. Association of the mammalian proto-oncoprotein Int-6 with the three protein complexes eIF3, COP9 signalosome and 26S proteasome. *FEBS Lett* **527:** 15–21.

Karniol B, Yahalom A, Kwok S, Tsuge T, Matsui M, Deng XW, Chamovitz DA. 1998. The *Arabidopsis* homologue of an eIF3 complex subunit associates with the COP9 complex. *FEBS Lett* **439:** 173–179.

Kaygun H, Marzluff WF. 2005. Regulated degradation of replication-dependent histone mRNAs requires both ATR and Upf1. *Nat Struct Mol Biol* **12:** 794–800.

Kolev NG, Steitz JA. 2005. Symplekin and multiple other poly-adenylation factors participate in 3′-end maturation of histone mRNAs. *Genes Dev* **19:** 2583–2592.

Kolev NG, Yario TA, Benson E, Steitz JA. 2008. Conserved motifs in both CPSF73 and CPSF100 are required to assemble the active endonuclease for histone mRNA 3′-end maturation. *EMBO Rep* **9:** 1013–1018.

LeFebvre AK, Korneeva NL, Trutschl M, Cvek U, Duzan RD, Bradley CA, Hershey JW, Rhoads RE. 2006. Translation initiation factor eIF4G-1 binds to eIF3 through the eIF3e subunit. *J Biol Chem* **281:** 22917–22932.

Ling J, Morley SJ, Pain VM, Marzluff WF, Gallie DR. 2002. The histone 3′-terminal stem–loop-binding protein enhances translation through a functional and physical interaction with eukaryotic initiation factor 4G (eIF4G) and eIF3. *Mol Cell Biol* **22:** 7853–7867.

Mack DL, Boulanger CA, Callahan R, Smith GH. 2007. Expression of truncated Int6/eIF3e in mammary alveolar epithelium leads to persistent hyperplasia and tumorigenesis. *Breast Cancer Res* **9:** R42. doi: 10.1186/bcr1742.

Marchetti A, Buttitta F, Miyazaki S, Gallahan D, Smith GH, Callahan R. 1995. Int-6, a highly conserved, widely expressed gene, is mutated by mouse mammary tumor virus in mammary preneoplasia. *J Virol* **69:** 1932–1938.

Martineau Y, Derry MC, Wang X, Yanagiya A, Berlanga JJ, Shyu AB, Imataka H, Gehring K, Sonenberg N. 2008. Poly(A)-binding protein-interacting protein 1 binds to eukaryotic translation initiation factor 3 to stimulate translation. *Mol Cell Biol* **28:** 6658–6667.

Masutani M, Sonenberg N, Yokoyama S, Imataka H. 2007. Reconstitution reveals the functional core of mammalian eIF3. *EMBO J* **26:** 3373–3383.

Morris C, Jalinot P. 2005. Silencing of human Int-6 impairs mitosis progression and inhibits cyclin B-Cdk1 activation. *Oncogene* **24:** 1203–1211.

Morris C, Wittmann J, Jack HM, Jalinot P. 2007. Human INT6/eIF3e is required for nonsense-mediated mRNA decay. *EMBO Rep* **8:** 596–602.

Morris-Desbois C, Bochard V, Reynaud C, Jalinot P. 1999. Interaction between the Ret finger protein and the Int-6 gene

product and co-localization into nuclear bodies. *J Cell Sci* **112:** 3331–3342.

Phan L, Zhang X, Asano K, Anderson J, Vornlocher HP, Greenberg JR, Qin J, Hinnebusch AG. 1998. Identification of a translation initiation factor 3 (eIF3) core complex, conserved in yeast and mammals, that interacts with eIF5. *Mol Cell Biol* **18:** 4935–4946.

Pick E, Hofmann K, Glickman MH. 2009. PCI complexes: Beyond the proteasome, CSN, and eIF3 Troika. *Mol Cell* **35:** 260–264.

Rasmussen SB, Kordon E, Callahan R, Smith GH. 2001. Evidence for the transforming activity of a truncated Int6 gene, in vitro. *Oncogene* **20:** 5291–5301.

Siridechadilok B, Fraser CS, Hall RJ, Doudna JA, Nogales E. 2005. Structural roles for human translation factor eIF3 in initiation of protein synthesis. *Science* **310:** 1513–1515.

Sullivan KD, Mullen TE, Marzluff WF, Wagner EJ. 2009a. Knockdown of SLBP results in nuclear retention of histone mRNA. *RNA* **15:** 459–472.

Sullivan KD, Steiniger M, Marzluff WF. 2009b. A core complex of CPSF73, CPSF100, and Symplekin may form two different cleavage factors for processing of poly(A) and histone mRNAs. *Mol Cell* **34:** 322–332.

Suo J, Snider SJ, Mills GB, Creighton CJ, Chen AC, Schiff R, Lloyd RE, Chang EC. 2011. Int6 regulates both proteasomal degradation and translation initiation and is critical for proper formation of acini by human mammary epithelium. *Oncogene* **30:** 724–736.

Townley-Tilson WH, Pendergrass SA, Marzluff WF, Whitfield ML. 2006. Genome-wide analysis of mRNAs bound to the histone stem–loop binding protein. *RNA* **12:** 1853–1867.

Watkins SJ, Norbury CJ. 2004. Cell cycle-related variation in subcellular localization of eIF3e/INT6 in human fibroblasts. *Cell Prolif* **37:** 149–160.

Yahalom A, Kim TH, Winter E, Karniol B, von Arnim AG, Chamovitz DA. 2001. *Arabidopsis* eIF3e (INT-6) associates with both eIF3c and the COP9 signalosome subunit CSN7. *J Biol Chem* **276:** 334–340.

Yen HC, Chang EC. 2000. Yin6, a fission yeast Int6 homolog, complexes with Moe1 and plays a role in chromosome segregation. *Proc Natl Acad Sci* **97:** 14370–14375.

Yen HC, Gordon C, Chang EC. 2003. *Schizosaccharomyces pombe* Int6 and Ras homologs regulate cell division and mitotic fidelity via the proteasome. *Cell* **112:** 207–217.

Zhao X, McKillop-Smith S, Muller B. 2004. The human histone gene expression regulator HBP/SLBP is required for histone and DNA synthesis, cell cycle progression and cell proliferation in mitotic cells. *J Cell Sci* **117:** 6043–6051.

Zhou C, Arslan F, Wee S, Krishnan S, Ivanov AR, Oliva A, Leatherwood J, Wolf DA. 2005. PCI proteins eIF3e and eIF3m define distinct translation initiation factor 3 complexes. *BMC Biol* **3:** 14. doi: 10.1186/1741-7007-3-14.

Zhou M, Sandercock AM, Fraser CS, Ridlova G, Stephens E, Schenauer MR, Yokoi-Fong T, Barsky D, Leary JA, Hershey JW, et al. 2008. Mass spectrometry reveals modularity and a complete subunit interaction map of the eukaryotic translation factor eIF3. *Proc Natl Acad Sci* **105:** 18139–18144.